PREPARATION OF TEMPO-CELLULOSE NANOFIBER/ZINC OXIDE AS ANTIMICROBIAL AND METHYLENE BLUE PHOTO-DEGRADING NANOCOMPOSITE

MOHAMED EL-SAKHAWY,[*] AHMED SALAMA,[*] AHMED K. EL-ZIATY[**] and HAZEM HASSAN[***]

[*]*Cellulose and Paper Department, National Research Centre, 33 El-Bohouth st., Dokki, P.O. 12622, Giza, Egypt*
[**]*Chemistry Department, Faculty of Science, Ain Shams University Abbassia, Cairo, Egypt*
[***]*Greater Cairo Sanitary Drainage Company (GCSDC), Central Labs, Cairo, Egypt*
✉ *Corresponding author: M. El-Sakhawy, elsakhawy@yahoo.com*

Received November 3, 2020

Photo-catalytic degradation of organic dyes in aquatic environments under visible light irradiation affords an efficient and economic technique for environmental remediation. TEMPO-oxidized cellulose nanofibers/zinc oxide nanocomposite (TEMPO-CNF/ZnO) was prepared through oxidation of cellulose pulp, followed by zinc oxide precipitation in the presence of oxidized fibers. TEMPO-CNF/ZnO was characterized by different techniques. The degradation rate of methylene blue (MB) by TEMPO-CNF/ZnO was gradually increased with increasing pH and the degradation reached 86% within 340 minutes at pH 7. The kinetic study showed that the pseudo-first-order kinetic best fitted the photo-catalytic process. A mechanism was proposed for the degradation of MB using TEMPO-CNF/ZnO under visible light irradiation. TEMPO-CNF/ZnO nanocomposite showed high antibacterial activity against *S. aureus* and *E. coli*. Thus, TEMPO-CNF/ZnO nanocomposite has been demonstrated to be effective photo-catalytic materials for degrading MB under visible light irradiation.

Keywords: TEMPO-oxidized cellulose, zinc oxide, composite, photo-degradation, dyes

INTRODUCTION

Photo-catalysis has emerged as a low-cost and facile strategy for the degradation of organic pollutants.[1] Metal oxides, such as zinc oxide and silver oxide, are the most commonly used photo-catalysts due to their photo-stability and interesting optical and mechanical properties. They harness the photo energy to produce active radicals that enhance the decomposition of organic pollutants.[2] Semiconducting materials can produce active hydroxyl radicals when the energy of the photon is higher than the energy gap of the semiconductor. This energy transfers the electrons from the valence band to the conducting band, creating a hole that can generate hydroxyl radicals in an alkaline medium. These radicals are highly reactive and can enhance the oxidation of recalcitrant chemicals in wastewater, leading to complete degradation of organic pollutants into nontoxic low molecular weight molecules (such as CO_2 and H_2O). The hydroxyl active radicals attack the organic materials via four different pathways: radical addition, hydrogen abstraction, electron transfer, and radical combination.[3] However, the commonly used semiconductors, such as TiO, ZnS and CdS, with a wide band gap, higher than 3.0 eV, can only absorb UV range light. Many studies were carried out for preparing highly efficient photo-catalysts, with narrower band gaps, which could well use the incident light to produce redox reactions. For example, ferromagnetic photo-catalysts have been studied for preparing the required optical absorption with relatively narrow band gaps (~2 eV). The magnetic field of ferromagnetic photo-catalysts enables their separation from wastewater and they can be recycled for further use. Narrow-band-gab semiconductors are currently needed to generate more electron−hole pairs under visible light. Moreover, the morphology has a significant effect on the charge carrier efficiency of semiconductor photo-catalyst.[4] Polysaccharides have been considered recently as host materials of metal oxides and inorganic nanoparticles.[5,6] They can enhance the stability, control the special morphology, and assist the growth of nanoparticles.[7,8] The exceptional features of metal nanoparticles, such as their electrical, magnetic, and optical properties, were preserved after immobilization on the polysaccharides. Metal nanoparticles/polysaccharides composite materials have been studied as a portable catalyst for water treatment,[9] antimicrobial material[10] and, recently, as a photo-catalyst.[1,11]

Cellulose nanofibers have several characteristics differing from those of conventional neat cellulose, such as specific surface area, special dimensions, morphology, crystallinity, and mechanical properties. Cellulose nanofibers based composites have a strong adsorption property and are a good candidate for wastewater treatment.[12] The oxidation of cellulose pulp through 2,2,6,6-tetramethyl piperidinyl-1-oxyl (TEMPO)-mediated oxidation is a promising process for preparing highly charged, carboxyl-functionalized cellulose nanofibers.[13] TEMPO is highly stable nitroxyl radical, which is used in selective oxidation of primary alcohols to corresponding carboxylic acid and aldehydes in the presence of a primary oxidizing agent, such as sodium hypochlorite.

Nanostructured oxides of metals, such as magnesium, tin, titanium, zirconium and zinc, have interesting and unique morphological properties, including size depending properties, such as the scaling of the energy gap with a change in the electrical and optical properties. For example, a cellulose nanofibers/titanium dioxide composite was prepared and evaluated for photocatalytic activity under UV light. Composite films of TiO_2–CNF were shown to be strongly photo-catalytically active in UV light, and subsequent modification with Au and Ag was displayed to improve their photo-catalytic efficiency in visible light.[14] Among nanostructured metal oxides, ZnO is considered as one of the most important oxide materials due to its specific properties. It is used in several applications, such as photo-catalysis, antibacterial materials, dyes and sensitized solar cells.[15,16] Several techniques have been applied to synthesize ZnO nanoparticles, such as the sol-gel method, vapor deposition, hydrothermal synthesis, thermal decomposition, precipitation, and spray pyrolysis.[17,18] For expanding its applications, numerous composites of ZnO have been broadly studied. Different studies investigated the synthesis of cellulose derivatives/ZnO composites. Cellulose and its derivatives act as structural templates in the design and preparation of zinc oxide nanomaterials with many structural varieties.[19] Cellulose derivatives/ZnO composite materials were applied to adsorb organic dyes and treat wastewater by destroying and breaking up organic pollutants.

The most successful demonstration for the treatment of wastewater was reported by using titanium oxide (TiO_2) and zinc oxide (ZnO).[20] However, zinc oxide is a more efficient photo-catalyst than TiO_2, because it has high reaction rates owing to its high efficiency to generate hydroxyl ions.[21] Moreover, ZnO enhances the possibility for visible-light photocatalytic activity.[22] For all these features, a cellulosic material/ZnO composite is a promising candidate to remove organic pollutants, such as dyes, from wastewater. In the current study, 2,2,6,6-tetramethylpiperidine-1-oxyl (TEMPO)-mediated oxidation was applied to produce TEMPO-CNF from cellulose pulp. Zinc oxide was prepared in the presence of oxidized cellulose fibers. The prepared TEMPO-CNF/ZnO was characterized and investigated as a photo-catalyst for organic pollutants from the wastewater, as well as an antimicrobial reagent to inhibit the growth of various bacteria and fungi.

EXPERIMENTAL

Materials

Bleached bagasse pulp was supplied by Qena Company of Paper Industry, Egypt. 2,2,6,6-tetramethylpiperidine-1-oxyl (TEMPO) and zinc sulfate heptahydrate were purchased from Sigma Aldrich. All other chemicals were of analytical grades and used without further purification.

Preparation of TEMPO-oxidized cellulose (TEMPO-CNF)

TEMPO-oxidized bagasse pulp was prepared through the dispersion of 20 g of bleached bagasse pulp in distilled water with TEMPO (0.8 g) and sodium bromide (8 g).[23] Then, 300 mL of sodium hypochlorite solution (15%) was added with continuous stirring and the pH was adjusted to 10 using NaOH solution. Then, the pH was adjusted to 7 and the oxidized fibers were centrifuged several times. Finally, TEMPO-CNF was dialyzed for 6 days. TEMPO-CNF was treated using a Masuko grinder as a mechanical defibrillation technique.

Synthesis of TEMPO-CNF/ZnO

The formed TEMPO-CNF was immersed in 50 mL of zinc sulfate heptahydrate solution 0.2M. Then, 1M NaOH solution was dropped into the solution until the pH reached 9 under continuous stirring at room temperature. The TEMPO-CNF/zinc oxide was formed by drying the precipitate at 90 °C for 48 hours, then sieved to separate only zinc oxide nanoparticles.

Characterization methods

The attenuated total reflectance Fourier transform infrared (ATR-FTIR) spectra of materials were obtained using a Thermo Nicolet FT-IR Avatar 320, with a diamond crystal, and the spectra were recorded from 500 to

4000 cm^{-1}. X-ray diffraction was performed with a scanning rate of 2θ = 2.5º/minute. Thermogravimetric analysis was accomplished with sensitivity measurements of 0.01 mg and 25 μv, respectively. In each run, 10 mg of sample was heated to 1273 K, at a heating rate of 283 K/min under N_2 flow at a rate of 30 mL/minute. Scanning electron microscopy was conducted at 5-10 keV at the National Research Center. Also, diffuse reflectance ultraviolet-visible spectroscopy (UV–vis DRS) of the samples was carried out at room temperature using a UV–vis UNICO UV-2000 in the range of 200-1000 nm.

Batch photo-catalytic degradation of MB

The photo-degradation of MB was conducted in 100 mL of solution placed in a Pyrex reactor. The MB solution was introduced into the photo-reactor in addition to 0.5 g of TEMPO-CNF/ZnO nanocomposite. After achieving the adsorption-desorption equilibrium, the sample was irradiated by visible light for a distinct time. During irradiation, agitation was maintained by an aerator to ensure a constant supply of oxygen and for stirring. 5 mL of sample was withdrawn from the bulk solution at predetermined time intervals and the degradation efficiency was determined by applying the following equation:

$$\text{Degradation efficiency (\%)} = [C_o - C_t / C_o] \text{ X } 100 \quad (1)$$

where C_o (mg L^{-1}) is the initial concentration dye and C_t (mg L^{-1}) is its concentration at the time, t. The concentrations of MB in the samples were determined and corresponding to the maximum absorption wavelength of MB. All the measurements were made in triplicate, with errors below 5%, and average values were reported. The adsorption was studied in visible light with continuous stirring during the photo-catalytic experiments. The decolorization was determined at the maximum wavelength of 630 nm.

Antimicrobial screening

The antibacterial activity of TEMPO-CNF and TEMPO-CNF/ZnO was tested against two types of bacteria: (i) gram-negative: *Escherichia coli* ATCC 11775, (ii) gram-positive: *Staphylococcus aureus* ATCC 12600, as well as against *Aspergillus flavus* and *Candida albicans* ATCC 7102 as models of filamentous fungi using nutrient agar medium. The sterilized medium, autoclaved at 120 °C for 30 minutes and incubated with one of the microorganisms, was put into a Petri dish to give a depth of 6.0 mm. The examined films, with a diameter of 1 cm, were placed on the seeded agar plate. After 24 hours of incubation at 37 °C, the diameters of the inhibition zones were measured.

RESULTS AND DISCUSSION

Characterization of TEMPO-CNF/ZnO nanocomposite

TEMPO-oxidation of cellulose pulp generates new carboxylic groups through selective oxidation of primary hydroxyl groups in the anhydroglucose units. The TEM image in Figure 1A displays TEMPO-CNF with the diameter in the range of 5-13 nm. These results were obtained previously in our work.[13] Moreover, the oxidized fibers have a uniform and homogeneous structure arising from the carboxylic groups, which assist the defibrillation of cellulose chains through the electrostatic repulsion force. Also, these groups could assist the cross-linking of the fibrils in different ways, such as the formation of intermolecular hydrogen bonding and supporting the formation of composites. In the current study, the carboxyl groups on TEMPO-CNF can be used to form a fully physically cross-linked nanocomposite with ZnO.

Morphological analysis of TEMPO-CNF before and after zinc oxide mineralization is shown in Figure 1. SEM images of TEMPO-CNF exhibit random spatial organization and a non-homogeneous distribution of fiber diameters. After zinc oxide precipitation, the surface morphology of the TEMPO-CNF/ZnO nanocomposite is relatively homogenous and the formed zinc oxide layer shows the presence of microplates with ~0.5 μm length. These plates appear to be distinct and uniform, likely due to the interaction between the TEMPO-CNF and the formed nanoparticles, which decreases the attractive forces among nanoparticles, reducing their aggregation tendency. Using bioactive cellulose to assist inorganic mineralization has been reported in the literature.[24]

TEMPO-CNF and TEMPO-CNF/ZnO nanocomposite were characterized by FTIR spectroscopy, as shown in Figure 2A and B. TEMPO-CNF exhibits a peak at 1160 cm^{-1} assigned to the C–O–C ether bonds, while the peak at 1630 cm^{-1} can be assigned to the carboxylate groups. The TEMPO-CNF/ZnO composite exhibits a characteristic band at 440 cm^{-1} due to the stretching mode of the zinc and oxygen bond, which confirms the presence of ZnO species in the final composite. Moreover, a peak at 1100 cm^{-1} may be attributed to C–O–C ether bonds. Also, a peak at 1623 cm^{-1}, corresponding to the carboxylate groups, could be related to the adsorption of carboxylate onto ZnO structures. The broadband at 3300 cm^{-1} is assigned to –OH stretching. Moreover, the FTIR spectrum of the TEMPO-

CNF gel exhibits a peak at 1160 cm^{-1}, corresponding to the C–O–C ether bonds, while the peak at 1630 cm^{-1} corresponds to the carboxylate groups.[25]

CNF was prepared and characterized by XRD in a previously published study.[26] The XRD pattern of the TEMPO-CNF/ZnO nanocomposite is shown in Figure 2C. The TEMPO-CNF/ZnO nanocomposite exhibits peaks at 2θ values of 32°, 34.1°, 35.2°, 46.3°, 58.6° and 62.7°, assigned to the ZnO crystal planes of (100), (002), (101), (102), (110), and (103), respectively, which are indexed to the hexagonal ZnO wurtzite structure (JCPDS no. 36–1451). The results suggested the successful formation of crystalline ZnO.

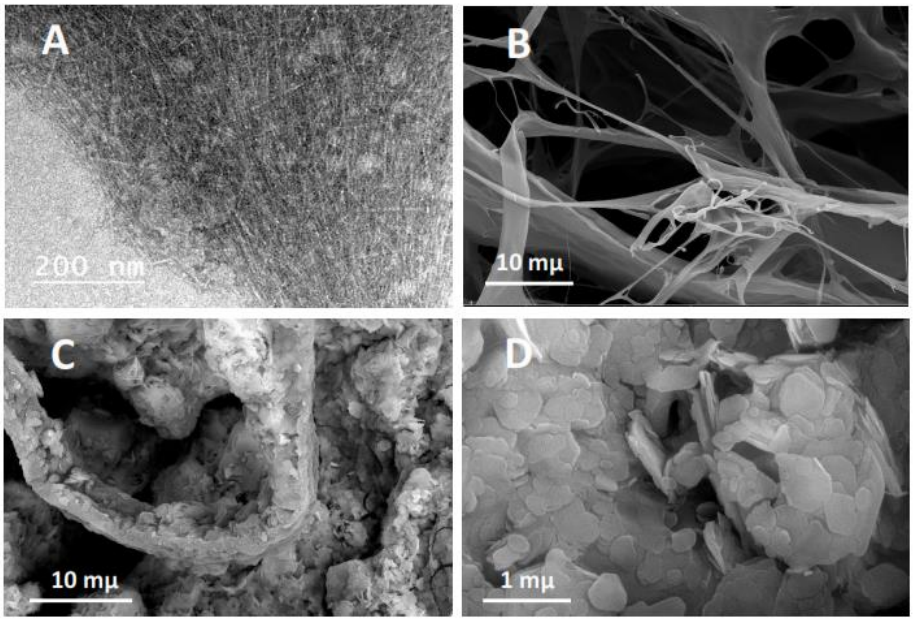

Figure 1: TEM image of TEMPO-CNF (A); SEM images of TEMPO-CNF (B) and TEMPO-CNF/ZnO nanocomposite at different magnifications (C and D)

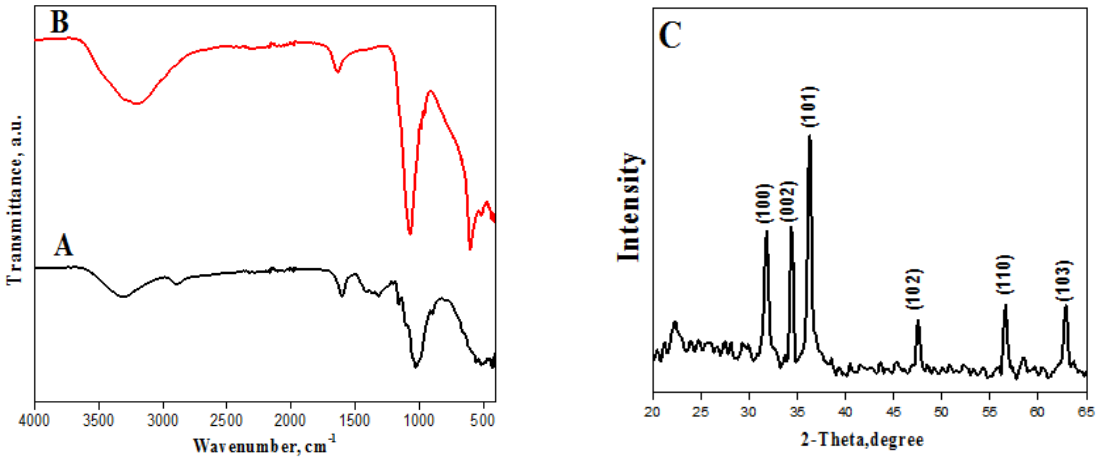

Figure 2: FT-IR spectra of TEMPO-CNF (A) and TEMPO-CNF/ZnO (B); XRD pattern of TEMPO-CNF/ZnO nanocomposite (C)

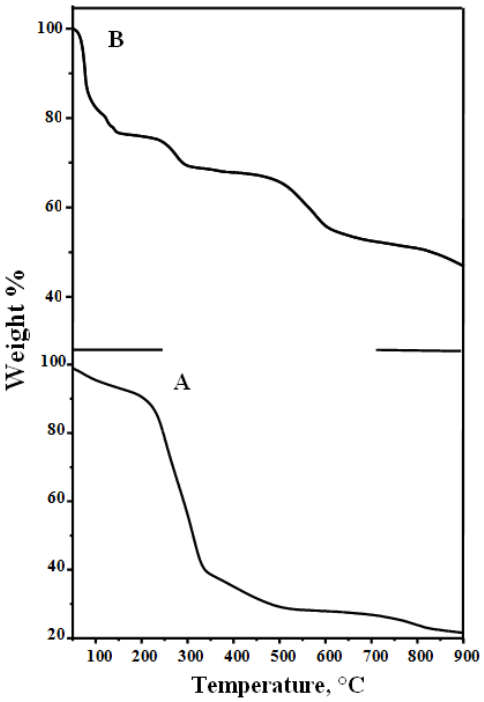

Figure 3: TGA curves of TEMPO-CNF (A) and TEMPO-CNF/ZnO (B)

The thermogravimetric curves of TEMPO-CNF and TEMPO-CNF/ZnO nanocomposite are shown in Figure 3. TEMPO-CNF and TEMPO-CNF/ZnO contain a layer of moisture, which is eliminated at 110 °C. The decomposition that can be seen in the thermogram curves of both TEMPO-CNF and TEMPO-CNF/ZnO between 250 and 300 °C was attributed to the decomposition of the cellulose fiber and the decomposition from 500 °C was attributed to the region of D-glucopyranose monomer and the thermal degradation of the organic part,[27] it reached 76% of the mass loss, leaving 24% residue for TEMPO-CNF.[28] However, the TEMPO-CNF/ZnO composite exhibits higher thermal stability, compared with pure TEMPO-CNF, along the whole studied temperature range, and shows a moderate steady degradation rate, without a sharp degradation peak between 200-400 °C, in contrast to pure TEMPO-CNF. This could be attributed to the presence of ZnO nanostructures that can disperse within the cellulose fibers and shield them. The highly thermo-stable inorganic nanomaterials can improve the thermal degradation temperature of cellulose. It is known that ZnO has thermal stability over 900 °C.[29] The estimated mass loss of TEMPO-CNF/ZnO composite was 54%, with a residual mass of 46%, due to the presence of the thermally stable ZnO particles.

Photo-catalytic degradation of MB using TEMPO-CNF/ZnO nanocomposite

The photo-catalytic activity of the TEMPO-CNF/ZnO nanocomposite under simulated sunlight was examined using MB as a model for organic dye. Adsorption was accomplished via the charge and roughness of the nanocomposite surface. The equilibrium adsorption of MB by TEMPO-CNF/ZnO nanocomposite was reached after 90 minutes. Then, MB degradation started by visible light irradiation. The effect of adsorption and photo-degradation by the TEMPO-CNF/ZnO nanocomposite on MB concentration is shown in Figure 4A. MB shows a major absorption band at 655 nm. The addition of TEMPO-CNF/ZnO nanocomposite to the MB solution under visible light illumination leads to an apparent reduction in absorption with a slight wavelength shift. The intensity at 655 nm decreases progressively in the course of the photo-degradation of MB via the aromatic ring opening.

The UV-visible light plays a vital role in nano-sized semiconductors that could be controlled by calculating the band gap energy. The optical band gap was confirmed by using the Tauc relation. The Kubelka-Munk function is applied to convert the diffuse reflectance into an equivalent absorption coefficient and is generally used to analyze the powder sample by the extrapolation of the linear portion of the graph between $[\alpha h\nu]^2$ versus photon energy ($h\nu$), as shown in Figure 5B. The optical band gap energy value of the TEMPO-CNF/ZnO nanocomposite is 2.94 eV, which is in the blue

region, compared to the bulk ZnO (3.3 eV). This could be referred to the additional sub-band-gap energy levels induced by the abundant surface and interface defects in the accumulated particles.[30] This variation of band gap is an important aspect of the photo-catalytic activity of the TEMPO-CNF/ZnO nanocomposite.

The pH of the medium is an important parameter in the heterogeneous photo-catalysis process. The role of pH on the rate of photo-catalytic degradation was studied in the pH range 2-7. The degradation rate gradually increased as the pH increased, due to the presence of excess OH^- anions that enhance the photo-generation of hydroxyl radicals and increase the rate of degradation, as shown in Figure 5A.

The time effect on the photo-catalytic performance of TEMPO-CNF/ZnO under visible light irradiation toward the photo-degradation of MB is shown in Figure 5B. The degradation is denoted as a relation between (C/Co) and irradiation time, where Co and C are the concentrations of MB at the initial time and at time t, respectively. From the results, it is clear that the degradation of MB reached 86% within 340 minutes when utilizing TEMPO-CNF/ZnO.

The rate constant values, k, of both pseudo-first-order and pseudo-second-order kinetic models were used to fit the experimental data. The linearized forms of the pseudo-first-order and pseudo-second-order are given in Equations (1) and (2):

$$(-)\ln\frac{Ct}{Co} = K_{obs}t \quad (1)$$

$$\frac{1}{Ct} - \frac{1}{Co} = K_{obs}t \quad (2)$$

where k_{obs}: rate constant and at time t (min), C_o: concentration at time 0, and C_t: concentration at a certain time.

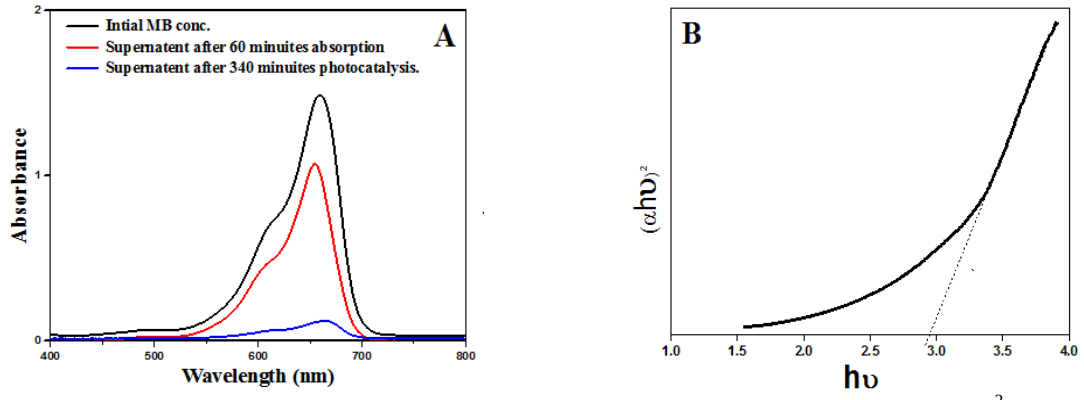

Figure 4: Adsorption and degradation contribute to lower MB concentrations (A); plots of $(\alpha h\nu)^2$ *versus* hν of TEMPO-CNF/ZnO nanocomposites (B)

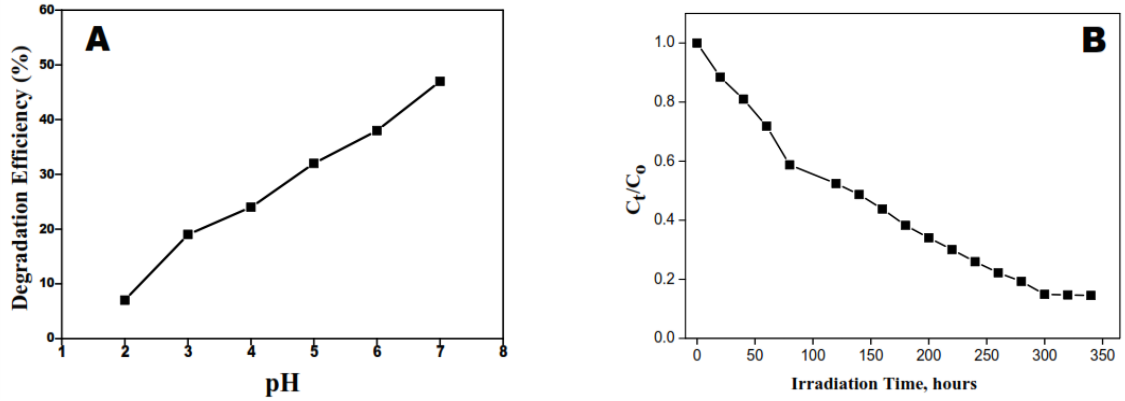

Figure 5: Effect of pH on photo-catalytic degradation at MB concentration: 20 ppm and TEMPO-CNF/ZnO dose: 0.5 g (A); Effect of time on photo-catalytic degradation of TEMPO-CNF/ZnO at MB concentration: 20 mg/L; TEMPO-CNF/ZnO: 0.5 g/50 mL and pH: 7.0 (B)

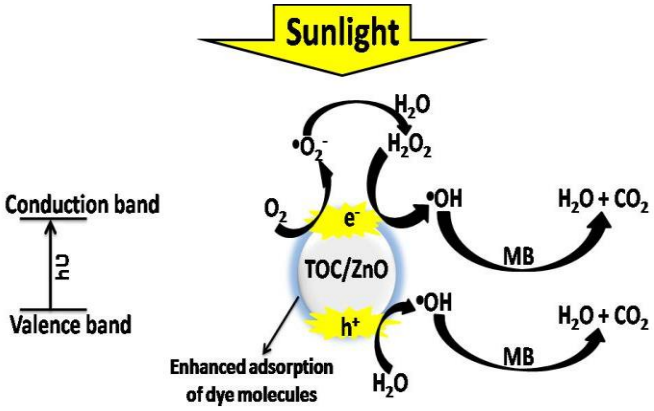

Figure 6: Mechanism of photo-catalytic degradation of MB by TEMPO-CNF/ZnO (TOC/ZnO)

The kinetic linear plots of (-) ln $\frac{Ct}{C0}$ *versus* t and $\frac{1}{Ct}$ - $\frac{1}{C0}$ *versus* t are drawn for the pseudo-first-order and pseudo-second-order models, respectively. The correlation coefficient obtained from the pseudo-first-order model (R^2 = 0.98) is higher than that from the other investigated model (R^2 = 0.88).

The mechanism of photo-catalytic activity of TEMPO-CNF/ZnO can be explained in terms of reactive oxygen species. TEMPO-CNF/ZnO is a semiconductor and it can generate electron-hole pairs after absorbing a photon. Low recombination between the excited electrons and holes is the significant characteristic of the TEMPO-CNF/ZnO to achieve good photo-catalytic activity. Briefly, when visible light is irradiated on TEMPO-CNF/ZnO, electrons from its valence band get excited to the conduction band, leaving holes behind. These photo-generated electrons are captured by dissolved O_2 in solutions to produce $O_2\bullet^-$ radicals. The thus obtained $O_2\bullet^-$ radicals can react with H^+ to produce H_2O_2, leading to the formation of $OH^\bullet$ radicals. Also, the photo-generated holes can react with H_2O and OH^- to produce OH• radicals. Thus, the generated reactive oxygen species (OH radicals) are responsible for the photo-degradation of the organic dye solution. The possible photochemical reactions taking place can be summarized in Figure 6.

Antimicrobial activity

Liu and Yang suggested that photo-catalytic oxidation enhanced the disinfection capability toward gram-positive and gram-negative bacteria in wastewater.[31] Isolated colonies of each organism were tested in terms of their susceptibility by the disc diffusion method. TEMPO-CNF exhibited low antibacterial activity (9 mm) against both *S. aureus* and *E. coli*. Moreover, there is no activity recorded against the fungi species. However, the TEMPO-CNF/ZnO nanocomposite has high antibacterial activity against both gram-positive and gram-negative pathogenic bacteria *S. aureus* and *E. coli* (Fig. 7 and Table 1). The inhibition zones for the TEMPO-CNF/ZnO nanocomposite against *S. aureus* and *E. coli* were of 28 and 23 mm, respectively. However, TEMPO-CNF/ZnO did not show antifungal activity toward *Aspergillus flavus*, while it showed moderate activity against *Candida albicans*. The inhibition zone against *C. albicans* was 14 mm. The antimicrobial activity of the ZnO nanocomposite is due to the reactive oxygen species produced by zinc oxide. Thus, the zinc ions released will attack the negatively charged bacterial cell wall and cause cell wall leakage. The higher reactivity of the nanocomposite toward *E. coli*, compared to *S. aureus*, may be attributed to the presence of a thick layer of peptidoglycans in the cell wall of *S. aureus*, compared to *E. coli*. The gram-negative bacteria have a structure of cell wall relatively more complex than that of gram-positive cells.[32] So, a longer oxidation time of the photo-catalyst would be required for inactivation of gram-negative bacteria by wall destruction during photo-catalytic inactivation. To conclude, the generated reactive oxygen species (OH radicals) are responsible for killing the bacteria.

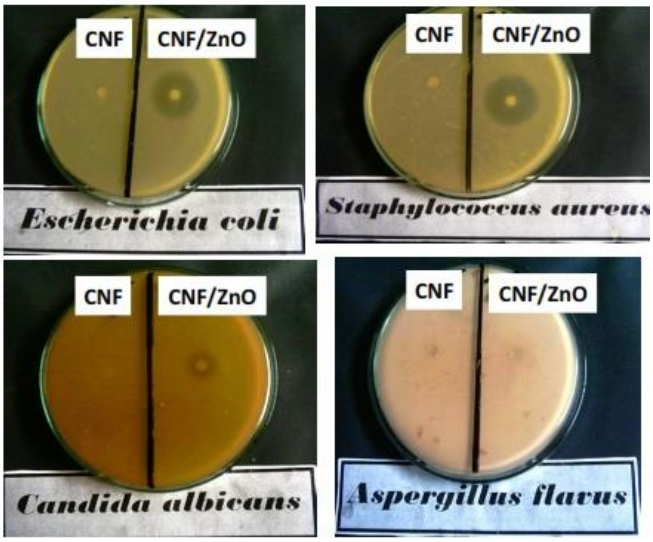

Figure 7: Antimicrobial activity of TEMPO-CNF and TEMPO-CNF/ZnO nanocomposite

Table 1
Antimicrobial activity of the synthesized TEMPO-CNF and TEMPO-CNF/ZnO nanocomposites

Sample		Inhibition zone diameter (mm/mg sample)			
		Escherichia coli (G^-)	*Staphylococcus aureus* (G^+)	*Aspergillus flavus* (fungus)	*Candida albicans* (fungus)
Standard	Ampicillin antibacterial agent	25	21	--	--
	Amphotericin B antifungal agent	--	--	17	21
Control: DMSO		0.0	0.0	0.0	0.0
TEMPO-CNF		9	9	0.0	0.0
TEMPO-CNF/ZnO		23	28	0.0	14

Table 2
Comparison of photo-catalytic degradation of MB by various photo-catalysts

Photo-catalyst	Percentage of degradation	Source of light	Initial conc. (mg/L)
ZnO prepared by precept[33]	81%	UV at 180 min.	20
ZnO prepared by sol-gel[33]	92.5%	UV at 180 min.	20
Cellulosic fibers coated with ZnO [34]	70%	UV at 480 min.	3
Cellulose/ZnO [35]	69.5%	Vis. at 60 min.	5
Cellulose/ZnO [35]	58.7%	Vis. at 90 min.	10
TEMPO-CNF/ZnO (current study)	86%	Vis. at 340 min.	20

Table 2 presents a comparative evaluation of available photo-catalysts for methylene blue dye. It can be observed that TEMPO-CNF/ZnO has better performance than other reported photo-catalysts. TEMPO-CNF/ZnO is a promising candidate photo-catalyst that can save energy and degrade dyes.

CONCLUSION

A novel sustainable TEMPO-CNF/ZnO nanocomposite was synthesized by oxidation of cellulose pulp, followed by zinc oxide precipitation. The TEMPO-CNF/ZnO nanocomposite exhibited excellent photo-catalytic activity in the degradation of MB under visible light irradiation and the degradation of MB reached 86% in 340 minutes. The developed material showed antibacterial activity against *S. aureus* and *E. coli*. Thus, the prepared TEMPO-CNF/ZnO nanocomposite has been demonstrated as an effective antimicrobial and photo-catalytic material for degrading MB under visible light irradiation.

ACKNOWLEDGEMENT: The authors would like to express their gratitude to the National Research Centre, Egypt, for the financial support of the current work.

REFERENCES

[1] G. Zhang, L. Chen, X. Fu and H. Wang, *Ind. Eng. Chem. Res.*, **57**, 4277 (2018), https://doi.org/10.1021/acs.iecr.8b00006
[2] R. Pandimurugan and S. Thambidurai, *Adv. Powder Technol.*, **27**, 1062 (2016), https://doi.org/10.1016/j.apt.2016.03.014
[3] C. Ren, B. Yang, M. Wu, J. Xu, Z. Fu *et al.*, *J. Hazard. Mater.*, **182**, 123 (2010), https://doi.org/10.1016/j.jhazmat.2010.05.141
[4] L. Gan, A. Geng, L. Xu, M. Chen, L. Wang *et al.*, *J. Clean. Prod.*, **196**, 594 (2018), https://doi.org/10.1016/j.jclepro.2018.06.086
[5] A. Salama and P. Hesemann, *Int. J. Biol. Macromol.*, **111**, 762 (2018), https://doi.org/10.1016/j.ijbiomac.2018.01.049
[6] M. El-Sakhawy, A. Salama, A. K. El-ziaty and H. Hassan, *Cellulose Chem. Technol.*, **54**, 601 (2020), https://doi.org/10.35812/CelluloseChemTechnol.2020.54.60
[7] A. Salama and P. Hesemann, *Int. J. Biol. Macromol.*, **147**, 276 (2020), https://doi.org/10.1016/j.ijbiomac.2020.01.046
[8] A. Salama, *Int. J. Biol. Macromol.*, **127**, 606 (2019), https://doi.org/10.1016/j.ijbiomac.2019.01.130
[9] J. Zeng, S. Liu, J. Cai and L. Zhang, *J. Phys. Chem. C*, **114**, 7806 (2010), https://doi.org/10.1021/jp1005617
[10] A. Salama, *Environ. Nanotechnol. Monit. Manag.*, **8**, 228 (2017), https://doi.org/10.1016/j.enmm.2017.08.003
[11] Q. Li, D. Zhou, P. Zhang, P. Man, Z. Tian *et al.*, *Colloid. Surfaces A Physicochem. Eng. Asp.*, **501**, 132 (2016), https://doi.org/10.1016/j.colsurfa.2016.04.054
[12] A. Salama, S. Etri, S. A. A. Mohamed and M. El-Sakhawy, *Carbohyd. Polym.*, **189**, 138 (2018), https://doi.org/10.1016/j.carbpol.2018.02.016
[13] A. Salama, R. E. Abou-Zeid, I. Cruz-Maya and V. Guarino, *Carbohyd. Polym.*, **229**, 115472 (2020), https://doi.org/10.1016/j.carbpol.2019.115472
[14] A. Snyder, Z. Bo, R. Moon, J. C. Rochet and L. Stanciu, *J. Colloid. Interface Sci.*, **399**, 92 (2013), https://doi.org/10.1016/j.jcis.2013.02.035
[15] W. L. Zheng, W. L. Hu, S. Y. Chen, Y. Zheng, B. H. Zhou *et al.*, *Chinese J. Polym. Sci.*, **32**, 169 (2014), https://doi.org/10.1007/s10118-014-1386-0
[16] H. Hassan, A. Salama, A. K. El-Ziaty and M. El-Sakhawy, *Int. J. Biol. Macromol.*, **131**, 520 (2019), https://doi.org/10.1016/j.ijbiomac.2019.03.087
[17] J.-H. Lee, K.-H. Ko and B.-O. Park, *J. Cryst. Growth*, **247**, 119 (2003), https://doi.org/10.1016/S0022-0248(02)01907-3
[18] Y. C. Kong, D. P. Yu, B. Zhang, W. Fang and S. Q. Feng, *Appl. Phys. Lett.*, **78**, 407 (2001), https://doi.org/10.1063/1.1342050
[19] H. Liu, Y. Zhang, H. Yang, W. Xiao and L. Sun, *J. Chem.*, **2016**, 1 (2016), https://doi.org/10.1155/2016/2862567
[20] A. Fujishima and T. N. Rao, *J. Chem. Sci.*, **109**, 471 (1997), https://doi.org/10.1007/BF02869207
[21] S. Baruah, M. Jaisai, R. Imani, M. M. Nazhad and J. Dutta, *Sci. Technol. Adv. Mater.*, **11**, 055002 (2010), https://doi.org/10.1088/1468-6996/11/5/055002
[22] S. Baruah and J. Dutta, *Sci. Technol. Adv. Mater.*, **10**, 013001 (2009), https://doi.org/10.1088/1468-6996/10/1/013001
[23] A. El-Gendy, R. E. Abou-Zeid, A. Salama, M. A. Diab and M. El-Sakhawy, *Egypt. J. Chem.*, **60**, 1007 (2017), https://doi.org/10.21608/ejchem.2017.1835.1153
[24] A. Salama and M. El-Sakhawy, *Int. J. Biol. Macromol.*, **92**, 920 (2016), https://doi.org/10.1016/j.ijbiomac.2016.07.077
[25] M. El-Sakhawy, S. Kamel, A. Salama and H.-A. S. Tohamy, *Cellulose Chem. Technol.*, **52**, 193 (2018), https://www.cellulosechemtechnol.ro/pdf/CCT3-4(2018)/p.193-200.pdf
[26] R. E. Abou-Zeid, A. Salama, Z. A. Al-Ahmed and N. S. Awwad, *Cellulose Chem. Technol.*, **54**, 237 (2020), https://doi.org/10.35812/CelluloseChemTechnol.2020.54.25
[27] H.-A. S. Tohamy, S. Kamel, M. El-Sakhawy, M. A. Youssef, A. E. M. Abdallah *et al.*, *Egypt. J. Chem.*, **63**, 3619 (2020), https://doi.org/10.21608/ejchem.2020.22915.2375
[28] M. El-Sakhawy, H.-A. S. Tohamy, A. Salama and S. Kamel, *Cellulose Chem. Technol.*, **53**, 667 (2019), https://doi.org/10.35812/CelluloseChemTechnol.2019.53.65
[29] F. Jones, H. Tran, D. Lindberg, L. Zhao and M. Hupa, *Energ. Fuels*, **27**, 5663 (2013), https://doi.org/10.1021/ef400505u
[30] A. K. Zak, R. Razali, W. H. Abd Majid and M. Darroudi, *Int. J. Nanomed.*, **6**, 1399 (2011),

https://doi.org/10.2147/IJN.S19693
[31] H.-L. Liu and T. C.-K. Yang, *Process Biochem*., **39**, 475 (2003), https://doi.org/10.1016/S0032-9592(03)00084-0
[32] S. A. A. Mohamed, M. El-Sakhawy and S. Kamel, *Cellulose Chem. Technol*., **52**, 423 (2018), https://www.cellulosechemtechnol.ro/pdf/CCT5-6(2018)/p.423-431.pdf
[33] A. Balcha, O. P. Yadav and T. Dey, *Environ. Sci. Pollut. Res*., **23**, 25485 (2016), https://doi.org/10.1007/s11356-016-7750-6
[34] M. H. Fallah, S. A. Fallah and M. A. Zanjanchi, *Chinese J. Chem*., **29**, 1239 (2011), https://doi.org/10.1002/cjoc.201190230
[35] A. Ali, S. Ambreen, Q. Maqbool, S. Naz, M. F. Shams *et al*., *J. Phys. Chem. Solids*, **98**, 174 (2016), https://doi.org/10.1016/j.jpcs.2016.07.007